applied sciences

MDPI

Article

Scenario-Based Pyroclastic Density Current Invasion Maps at Poorly Known Volcanoes: A Case Study from Changbaishan (China/North Korea)

Anna Maria Lombardi [1], Pierdomenico Del Gaudio [1], Zhengfu Guo [2], Maoliang Zhang [2,3], Guoming Liu [4,5], Vincenzo Sepe [1], Jiaqi Liu [2] and Guido Ventura [1,*]

1 Istituto Nazionale di Geofisica e Vulcanologia, 00143 Roma, Italy; annmaria.lombardi@ingv.it (A.M.L.); piero.delgaudio@ingv.it (P.D.G.); vincenzo.sepe@ingv.it (V.S.)
2 Key Laboratory of Cenozoic Geology and Environment, Institute of Geology and Geophysics, Chinese Academy of Sciences, Beijing 100029, China; zfguo@mail.iggcas.ac.cn (Z.G.); mzhang@tju.edu.cn (M.Z.); liujq@mail.igcas.ac.cn (J.L.)
3 Institute of Surface-Earth System Science, Tianjin University, Tianjin 300072, China
4 Earthquake Administration of Jilin Province, Changchun 130022, China; cbslgm@126.com
5 Changbaishan Volcano Observatory, Antu 133613, China
* Correspondence: guido.ventura@ingv.it

Received: 6 March 2020; Accepted: 7 April 2020; Published: 10 April 2020

Featured Application: Volcanic hazard evaluation, Urban Planning.

Abstract: Changbaishan volcano (China/North Korea; last eruption in 1903 AD) was responsible for a Volcanic Explosivity Index (VEI) 7 eruption in 946 AD. Approximately 186,000 people live around Changbaishan and 2,000,000 tourists/year visit the volcano. An unrest occurred between 2002 and 2006. Despite the relevant hazard, the eruptive history is poorly known, a condition common to many volcanoes worldwide. Here, we investigate the extension of the areas potentially affected by pyroclastic density currents (PDCs) in case of future eruptions following a scenario-based approach. We perform energy cone runs referred to four scenarios from columns of height 3, 10, 20 and 30 km at different vents. By using global datasets on PDCs, we produce spatial probability maps of PDCs invasion. Empirical laws between covered areas, PDC travelled distances, and heights of collapse are provided. In scenarios 3 and 4, PDCs expand at distances up to 42 km and 85 km, respectively. In scenarios 1 and 2, PDCs invade the touristic area and few main roads. Severe effects emerge from scenarios 3 and 4 with the interruption of the China–North Korea land and aerial connections and PDC. Our approach may serve as guide for the rapid evaluation of the PDC-related hazard at poorly known volcanoes.

Keywords: volcano; hazard; pyroclastic density currents; urban infrastructures; Changbaishan volcano

1. Introduction

Pyroclastic density currents (PDCs) may cover large distances in short times (few minutes to hours) [1–5]. PDCsform by different mechanisms including the collapse of eruptive columns or domes [6,7], blasts associated to the depressurization of the volcano flanks [8], and syn-eruptive gravitational collapse of hot pyroclasts accumulated over steep slopes [9]. The flow behavior and the emplacement mechanisms of PDCs havebeen reconstructed from field studies [10,11], direct observations [12] as well as numerical and experimental models [13–17]. These studies evidence the complex dynamics of PDCs highlighting the role of different factors (topography, temperature, degree of dilution, humidity) in controlling the path, velocity, impact, and area covered by PDCs.

With respect to other types of volcanic hazards, PDCs may produce several damages and fatalities at long distances from the vent area: PDCs and mud-flows account for 56% of life loss in the volcanic fatalities according to historical record [18,19]. The hazard evaluation related to PDCs suffers of the incomplete understanding of many, often variable, physical parameters associated to these flows; this limits our ability to exactly predict the flow paths and to estimate the extension of areas potentially covered by PDCs. Different empirical and physical models have been developed to determine the flow paths, areas of invasion, thickness variations, and velocity of PDCs. Among these, VolcFlow [20], LAHARZ [21], TITAN2D [22], energy cone (EC) [23] are more widely applied to PDCs hazard evaluation. In a review of these different models, [24] show that LAHARZ and EC can be used as first-approximation of flow runouts using the parameters listed in the FlowDat database [25] and other general or local databases [26–28]. In addition, these models may provide simple hazard maps when run with a variety of input volumes. However, they do not include the probability of occurrence. TITAN2D and VolcFlow are efficient in producing scenario-based or probabilistic hazard maps, but they need to run many times with varying input parameters. They are efficient to simulate single pulse, smaller-volume flows, whereas they are less sensitive in reproducing larger-volume flows. These latter models require a systematic calibration of input parameters, a feature that implies the acknowledgement of physical data (e.g., basal friction, retarding stress) not always available for many volcanoes. EC model is less sensitive to these parameters, is relatively efficient in reproduce large volume flows, but it is less sensitive in reproducing channelized flows. However, according to references [24,29], for a scenario-based approach to hazard evaluation from PDCs invasion, the energy cone model can be successfully applied [28–31]. The hazard associated to PDCs in poorly known volcanoes is difficult to evaluate because field constraints are few or lacking. However, Ogburn et al. [32] suggest that, in these cases, it is realistic to assume that a particular volcanic occurrence, e.g., a PDC from column collapse, while not the same across all the volcanoes, is controlled by comparable processes. Therefore, we can reasonably assume that, as in the case of PDCs [24], a volcanic occurrence varies according to some statistically representative laws. This implies that (a) the information from global databases is representative of a general behavior, and (b) a such behavior could be used for hazard assessment studies at a particular volcano. Here, we apply the EC model to construct scenario-based probability maps of PDCs area invasion and runout distances at Changbaishan volcano (2774 m; China/North Korea), also known as Paektu, Baekdu, Baitou, and Tianchi (Figure 1). The historical and recent eruptive history of Changbaishan is surprisingly poorly known although the volcano was responsible for a VEI ~7 Plinian eruption (Millennium eruption; 946 AD; Oppenheimer et al. [33]), which produced about 100 km^3 of tephra [34–37]. Changbaishan has been also affected by an unrest episode characterized by uplift, increased seismicity and changes in gas geochemistry between 2002 and 2006 [38]. In this study, we use data from the Flowdat PDC global database [24,25] and EC simulations [23] to identify the PDC inundation zones at Changbaishan volcano according to four selected reference scenarios representative of small-intermediate to Plinian eruptions [39] from different vents. We produce scenario-based probability maps superimposed to the Digital Terrain Model for the volcano and to the urban and infrastructural network (road, cities, railways, dams, airports). On the basis of the results from the EC runs and the probability maps we discuss the effects of different vent location and the morphology on the PDC invasion areas and extract some empirical relations between input and output parameters (e.g., collapse heightvs.PDC inundation area). The hazard implications are discussed. The analytical scheme we adopt may be applied to other volcanoes characterized by a relevant potential hazard and a poorly constrained eruptive history.

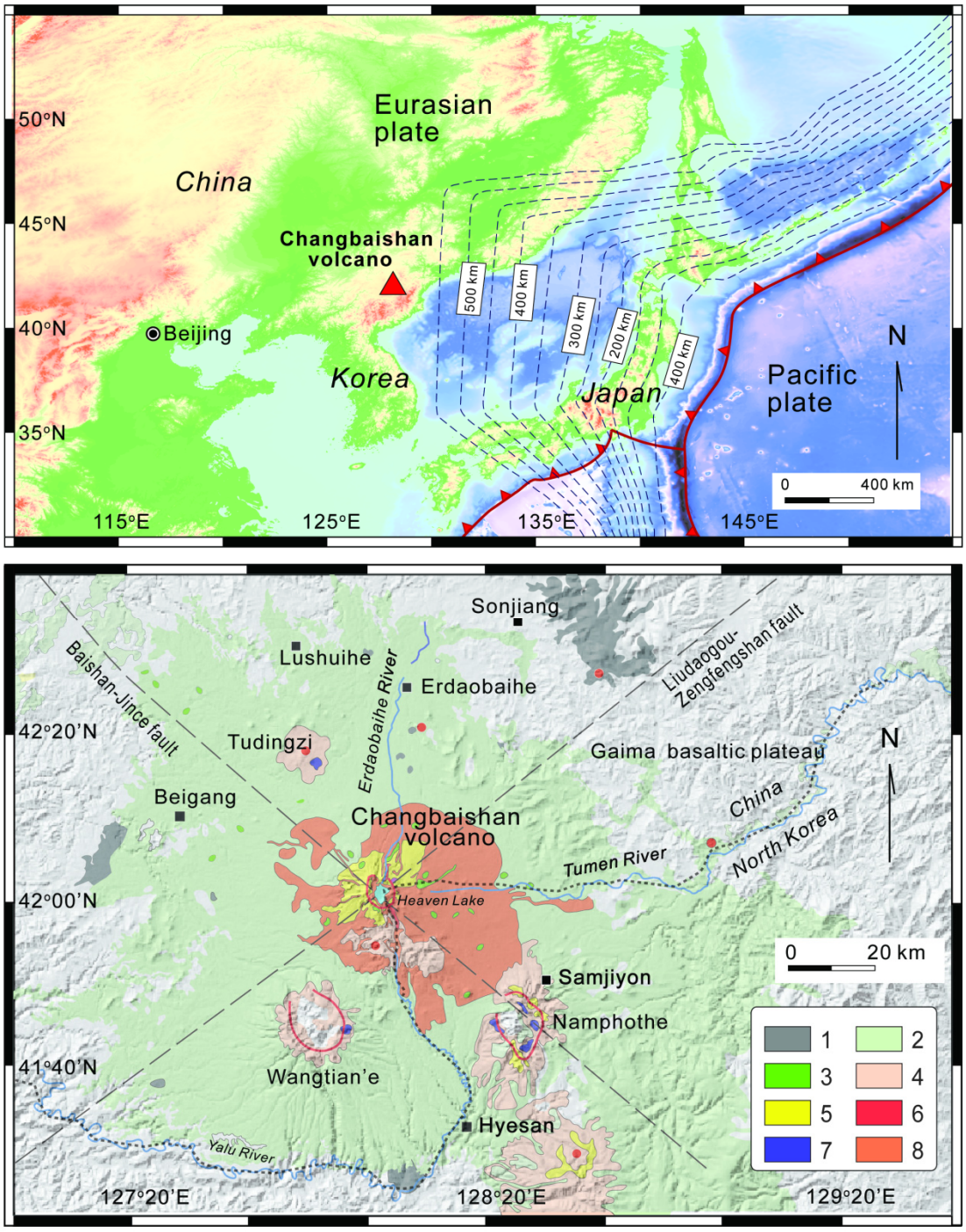

Figure 1. Top: geodynamic framework and location of the Changbaishan volcano. The digital elevation model is from https://maps.ngdc.noaa.gov/viewers/wcs-client/. The dashed lines show the depth contours of the subducting Pacific slab estimated from seismicity. Bottom: simplified geological map of the Changbaishan area superimposed to the ASTER GDEM V2 elevation model (https://asterweb.jpl.nasa.gov/gdem.asp). The main units are: 1, pre-shield basalts; 2, shield basalts; 3, post-shield basalts; 4, intermediate to silicic volcanic rocks (trachyte with minor trachyandesite); 5, intermediate to silicic volcanic rocks (trachyte with minor trachyandesite); 6, rhyolite 1; 7, rhyolite 2; 8, pyroclastic deposits related to caldera-forming eruptions. Blank area represents country rocks or sediments.

2. Geological and Volcanological Setting of the Changbaishan Volcano

Changbaishan volcano (2774 m; ~2 Ma-present) is the largest active volcano of China and lies above the flat portion of the Pacific slab subducting below the Eurasian plate (Figure 1). The volcano is located on the China-North Korea boundary and represents an intraplate, alkaline edifice with a summit caldera filled by a ~5 km wide, 300 m deep lake (Heaven Lake) [40,41]. A valley located in the northern flank, where the caldera rim is breached, hosts the only water outlet of the Heaven Lake. Such outlet forms the Erdaobaihe River (Figure 1). Changbaishan volcano lies on the Gaima basaltic plateau (29 Ma), which has an average altitude of 900–1000 m and covers the Sino-Korean Craton (Figure 1) [36,42], and it is the northernmost edifice of a group of volcanoes including the 5 to 2 Ma old Wangtian'e and Namphothe strato-volcanoes and smaller scale monogenetic centers [41,43]. The Changbaishan truncated cone has a basal diameter of about 50 km with radial valleys partially modified by glacial processes. Pre-caldera and post-caldera vents are located within and outside the present-day caldera depression (Figure 2).

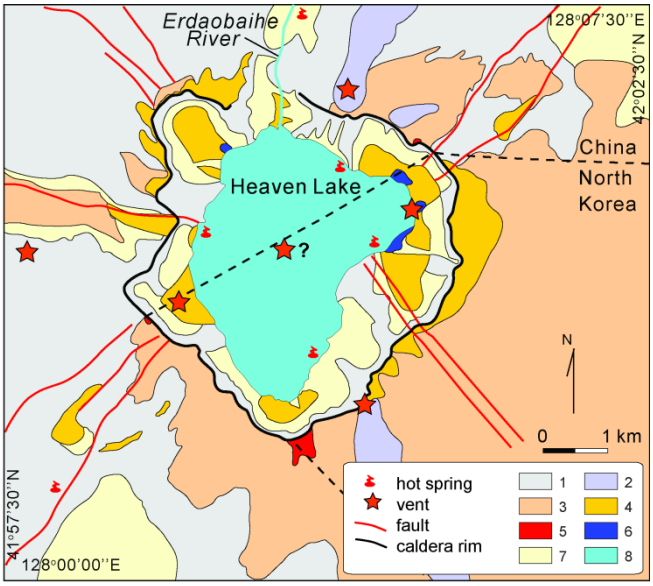

Figure 2. Simplified geological map of the Changbaishan caldera: 1, trachyte lava flows; 2, rhyolite lava flow; 3, Millennium eruption (946 AD) pyroclastic deposits; 4, 1668 AD pyroclastic deposits; 5, 1702 AD pyroclastic deposits; 6, 1903 AD pyroclastic deposits; 7, rock and debris flows; 8, water table and river.

The Changbaishan activity is divided in three main stages: a 2–1 Ma old basaltic shield formation stage, a trachytic to rhyolitic composite cone formation stage (1–0.04 Ma), and the latest, caldera-forming explosive stage (Figure 1) [36,43,44]. The Changbaishan caldera formed by a collapse event related to the VEI ~7, Millennium eruption (946 AD) [33], which ejected tephra of rhyoltic and trachytic composition (DRE ~25 km^3) [34,35,37,40]. Other explosive eruptions occurred in Holocene times. These include the 8.1 ka pre-Millennium Plinian Qixiangzhan eruption, and the post-Millennium eruptions recorded in historical documents and recognized in distal tephra (1403, 1668, and the VEI ~5 1702 AD) [42,45–49]. Wei et al. [36] report that the last eruption at Changbaishan occurred in 1903 AD within the summit caldera lake, however, Pan et al. [37] ascribe the intra-caldera deposits of this event and the proximal deposits of the 1668 and 1702 AD eruptions to the final part of the Millennium eruption. This problem causes a difficulty in evaluating the volcanic hazard correctly [36]. Ash fall deposits of the Millennium and Qixiangzhan eruptions and of the 1215, 1403, 1668 AD eruptions have been found in the lakes around Changbaishan. For the Plinian events, fall deposits have been found in the Japan Sea, Japan mainland and Greenland (Millennium eruption) [49,50]. The PDC deposits of Changbaishan, which frequently cover the fallout layers of the major eruptions, mainly outcrop in river gorges being significantly removed by fluvial and glacial erosion, and rainfall. A map of the spatial

distribution of PDC deposits at Changbaishan is, at the present, not available. The few outcrops allow us to estimate that PDCs cover an area of about 2430 km^2 [51]. The PDC deposits of the Millennium eruption can be traced 50–80 km away from the Changbaishan caldera [46,51]. In the valleys around the volcano, most PDCs evolve to lahars [51]. These latter have been found at distances up to 83 km north of the Changbaishan caldera. As concerns the next, possible eruption, the emplacement of fall and PDCs deposits with volumes of erupted magma in the range of 0.1–0.5 km^3, i.e.,VEI~ 3–4, is expected [36]. However, gravity and tomographic models [52,53] show that two low Vs, low density 50 km (width) × 5 km (height) and 20 km × 2.5 km sills occur at about 18 and 10 km depth. The dimension of these sills suggests the occurrence of magma chambers with a volume comparable to that responsible for the Millennium eruption. Therefore, a future eruption with VEI ~ 5–7 cannot be a priori excluded, also taking into account the poorly known eruptive history of the volcano [37]. Changbaishan was affected by an unrest episode between 2002 and 2006 [38] with hundreds of shallow earthquakes with M_L,max = 4.4. They were accompanied by ground uplift, increase of CO_2, He, H_2, and high $^3He/^4He$ possibly related to the refilling of a magma chamber. The 2002–2006 unrest has moved the Chinese and South Korea scientific communities to evaluate the potential hazards. According to Wei et al. [40,54], different hazards characterize the Changbaishan volcano. Avalanches, rock falls, and debris flows, mainly from the inner, steep caldera walls, and explosive interaction between magma and water, as well as CO_2 bursts, and Nyos-like events are well recognized hazards related to the occurrence of the Heaven Lake. Lahars, floods, and rock avalanches associated to the partial water withdrawal by overflows from the lake are also recognized as a primary source of hazard. Other relevant hazards include earthquakes and the emplacement of ash fall and PDCs. The evaluation of the hazard related to ash dispersion and PDC is of primary importance because about 135,000 people of China and 31,000 of North Korea live within 50 km from the Changbaishan caldera, and each year, 2,000,000 tourists visit the Changbaishan volcano National Reserve, a part of the UNESCO Man and Biosphere program [55] (http://www.stats.gov.cn/english/statisticaldata/censusdata/) [56]. In this framework, Lee et al. [57] and Yu et al. [58,59] model the ash dispersion for eruptions with VEI up to 7 and show that, due to the prevailing winds, ash deposition may heavily affect China and North Korea, with also consequences for the aviation routes and agricultural areas in South Korea and north Japan. Yun et al. [60] and Paone and Yun [61], by using the results of TITAN2 simulations for VEI 3 eruptions from 7 vents located along a NE-SW strike inside and outside the Changbaishan caldera, show that PDCs may deposit both inside and outside the caldera to a maximum distance of 7 km from the vent, mostly in the north valley hosting the Erdaobaihe River (Figure 1). In summary, with all the above discussed uncertainties regarding the eruptive activity of the volcano in historical times and the poorly known distribution of PDC deposits, some constraints are available and may be used as a guide for a scenario-based evaluation of the PDC hazard.

3. Analytical Methods

The EC model [23] extends the energy line model of Heim [62]. It bases on the conversion of potential energy of pyroclastics emitted from a vent of height H_{vent} into kinetic energy as the gravity-driven, cohesionless PDC moves away from the vent. When the energy is fully dissipated by frictions PDC stops. The height of column collapse above the vent is H_0 and H_t is the total height of the eruptive column measured from the altitude of the vent [23,28,30,31]. The angle of the energy line (ϕ) reflects the PDC's resistance to move and it is related to H_{vent}, H_0, and the distance travelled by PDC L, by:

$$\Delta H = H_{vent} + H_0 \text{ with} \rightarrow H_0 = 0.1\ H_t \quad (1)$$

$$\Delta H/L = \tan(\phi) \quad (2)$$

The energy cone model determines the energy lines on a digital elevation model (DEM) all around the vent area and the results are better constrained for relatively diluted PDC and less constrained for channelized flows. However, Changbaishan volcano shows, like Vesuvius volcano in

Italy, a cone-like morphology with PDC deposits radially emplaced around the volcano. According to ref. [31], these features should not affect the results, although a quantification of the uncertainties and a full validation cannot be done on the basis of the available field data. The advantages of the energy cone model are, for various reasons, the ability to perform several runs in relatively short time and to determine the areas covered by large volume flows [24]. In addition, the variability of PDCs may be indirectly taken into account by varying ΔH/L [27], which is a function of the volume of the erupted products, by maintaining constant the value of H_0. To evaluate the areas of potential PDC invasion at Changbaishan, we follow a scenario-based approach by varying the vent location, and by selecting columns of different height. We select 17 vents located at the center of the caldera and around the rim inside and outside the caldera depression (see Figure 3). This is because eruptive vents located both inside and outside the caldera have been recognized in the geological record (Figure 2) [36]. We assume that PDCs originate by column collapse and exclude the occurrence of dome collapse or blasts associated to the depressurization of the volcano flanks because domes or weakness zones on the volcano flanks are lacking and not recorded in the past history of the volcano. We also exclude the possible effects of winds on the eruptive column whose collapse may generate pyroclastic PDC. For each of these vents, we select four reference scenarios with column heights Ht of 3 km (scenario 1), 10 km (scenario 2), 20 km (scenario 3) and 30 km (scenario 4). The EC runs are performed by using the G-EVER routine of Takarada [29] (http://volcano.g-ever1.org/vhazard/HazardAssessment/). These Ht values are representative of events with VEI ~ 2–7 [39,63,64]. For each Ht, we select different values of ΔH/L as a function of the volume V of the erupted products on the basis of the relation ΔH/L = 0.11 ($V^{-0.14}$) [24], which is based on the FlowDat global database [25]. In particular, we select the best median ΔH/L value and the values of the upper and lower 95% prediction limits of the above reported relation (see Figure 2 of [24]). The selected ΔH/L values of each scenario, which are reported in Table 1, take into account the PDCs with the following ranges of volume: 10^{-4} to $10^{-1.7}$ km^3 (scenario 1), 10^{-3} to $10^{-0.8}$ km^3(scenario 2), 10^{-2} to $10^{0.3}$ km^3 (scenario 3), and $10^{-0.1}$ to $10^{1.77}$ km^3 (scenario 4). These variation ranges are within those estimated by [63] for eruptions with different VEI and column heights. Therefore, the three ΔH/L values, we adopt for each scenario account for the large uncertainties of the relations between Ht and PDCs volumes and for the different mobility of the flows, being smaller volume flows less mobile than the larger ones ([32] and reference therein). The reference DEM of Changbaishan volcano and surrounding areas used for the EC runs is the 30-m resolution ASTER GDEM V2 elevation model (https://asterweb.jpl.nasa.gov/gdem.asp). In total, we perform 204 runs, 51 for each scenario, and produce the relative invasion maps. We describe the uncertainty about the distribution of sites where PDCs may deposit by estimating the conditional spatial probability that PDCs arrive in a specific site. We assume that all the scenarios have the same probability of occurrence. This simplifying assumption bases on the observation that the available field and chronological data do not allow us, at the present, to determine possible recurrence times or to identify repose time-volume of erupted products relations at Changbaishan. As a result, the spatial probability values, which range from 0 to 1, are computed for each scenario as the proportion of times that a given area is covered by PDCs on the basis of 51 runs.

Table 1. Summary of the parameters used in the EC runs for each scenario. The minimum (min), median (med), and maximum (max) ΔH/Lvalues are selected according to the relationΔH/L= 0.11 ($V^{-0.14}$) of Ogburn and Calder [24] and correspond to the lower 95% prediction limit, the best-fitting value, and upper 95% prediction limit.

Scenario	Ht (m)	ΔH/L Min	ΔH/L Med	ΔH/L Max
1	3000	0.19	0.30	0.40
2	10,000	0.14	0.22	0.30
3	20,000	0.10	0.16	0.22
4	30,000	0.06	0.11	0.15

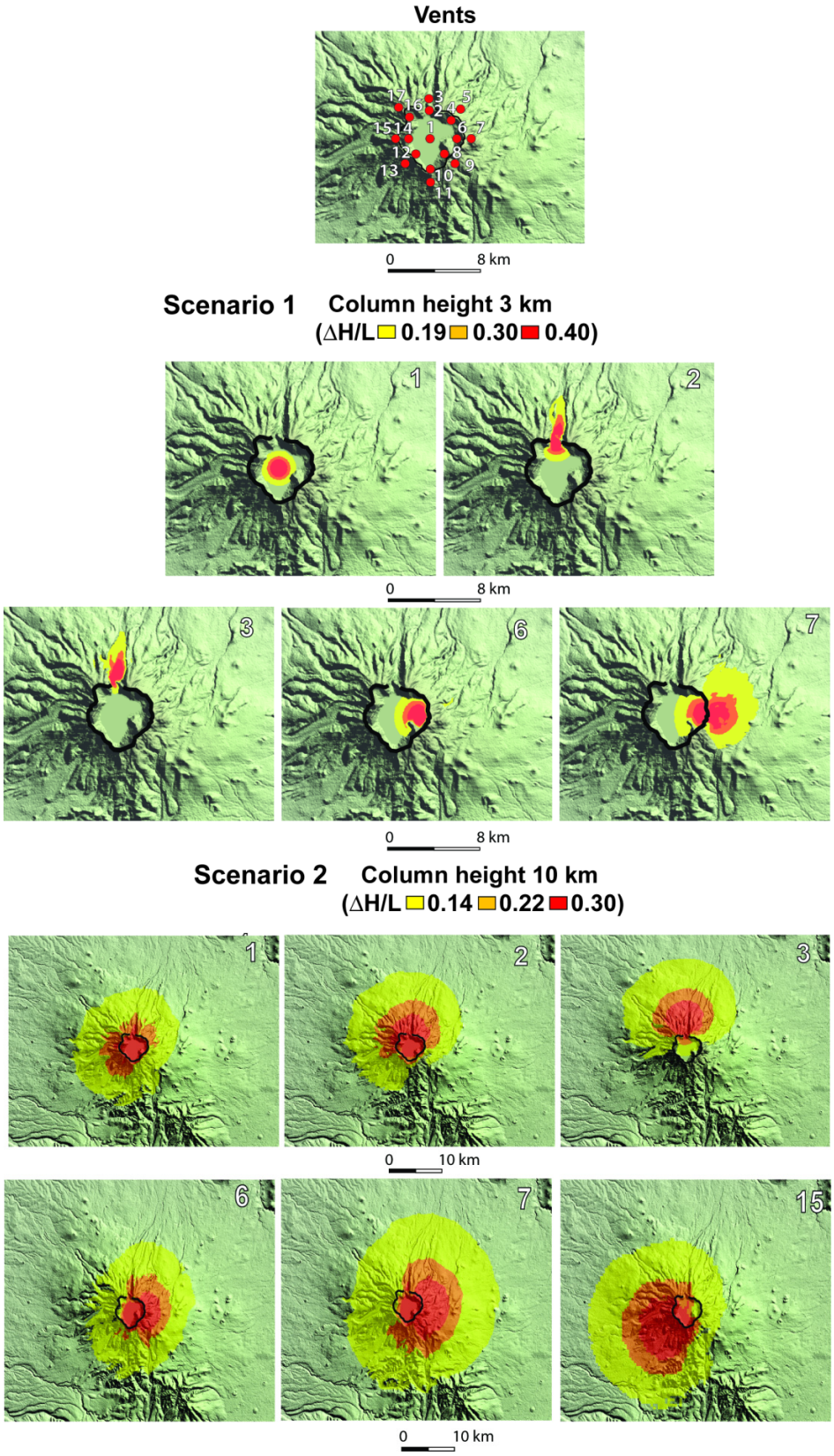

Figure 3. Top: location of the vents used for the simulations of the scenarios 1–4 and examples of EC simulations in scenario 1 (column height = 3 km) from different vents (white number in the panel) and three selected ΔH/L values. Bottom: examples of simulations in scenario 2 (column height = 10 km) from different vents (white number in the panel) and three selected ΔH/L values.

4. Results

Examples of the PDC invasion maps for the different scenarios and vent positions are reported in Figures 3 and 4. In scenario 1, these maps show that the PDC invasion area is partly controlled by the presence of the caldera rim (Figure 3). In particular, PDC are confined within the caldera for vents located in the inner side of the caldera (vents 1 and 6). PDC invasion area of vent 2, which is located within the caldera but close to a zone where the rim is interrupted and the caldera is open toward the north, manly covers the valley located in the northern flank of the volcano and, with a less extension, the caldera floor. The PDC invasion areas related to vents 3 and 7, both located outside caldera, mainly cover the flanks of the volcano, and, in a lesser amount, the inner caldera floor. The distance covered by PDCs in scenario 1 does not exceed about 7 km from the respective vent. This result is consistent with that obtained from TITAND2 simulations by Yun et al. [60] from six vents with a similar position with respect to the caldera rim and column height of 2–5 km. As concerns scenario 2, the PDC invasion area mainly affects the flanks of the volcano and, depending on the vent position, covers different sectors of the volcano (Figure 3).

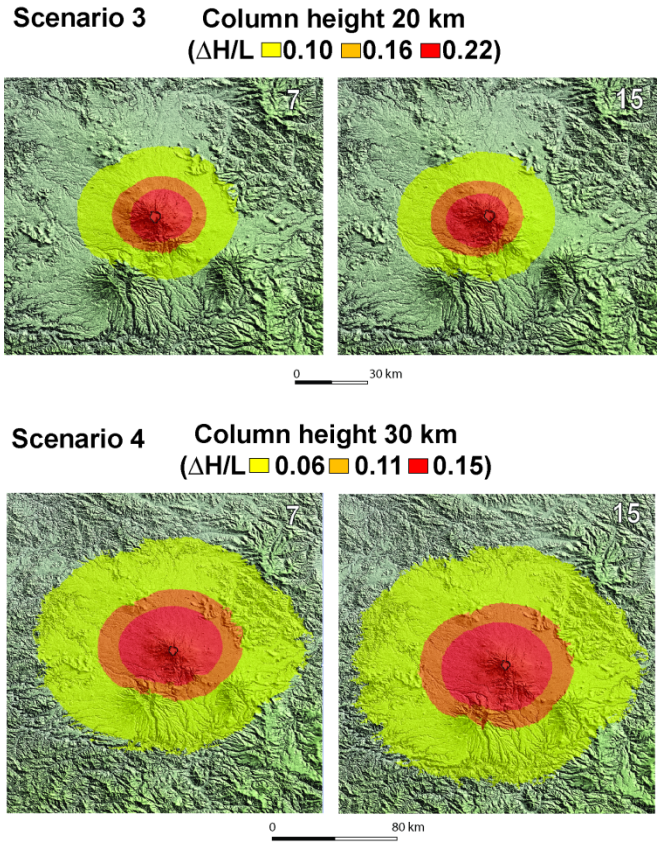

Figure 4. Top: examples of EC simulations in scenario 3 (column height = 20 km) from different vents (white number in the panel) and three selected ΔH/L values. Bottom: examples of simulations in scenario 4 (column height = 30 km) from different vents (white number in the panel) and three selected ΔH/L values.

The caldera floor is always covered by the PDCs. The maximum runout distance from the runs with the smaller ΔH/L value is in the order of 16–20 km, depending on the vent position. The distance from the runs with the larger ΔH/L does not exceed 10 km (Figure 3). The results of scenario 3 show that the distance variesfrom 28 to 37 km for the smallest ΔH/L value, whereas it is in the order of 12–15 km for the largest ΔH/L. In scenario 3 runs, significant effects of the vent position on the PDC dispersion areas are lacking. In scenario 4, the distance of PDCs determined for the smaller ΔH/L is of

80–85 km (Figure 4), a value corresponding to the maximum distance of 83 km measured in the field for the pumice-rich PDCs of the Millennium eruption [51,61].

The maximum distance travelled by PDCs from the runswith the smallest ΔH/L is between 35 and 40 km from the vent. The probability (p) invasion maps are shown in Figures 5–8. As expected, the more relevant feature of resulting probability maps is that the area of invasion and p increases with Ht. Low p-values (≤0.5) and a dependence of invasion probability map from the vent location may be recognized in scenario 1 (Figure 5). For higher Ht (Scenarios 2–4; Figures 6–8), the probabilities of invasion reach 1 in the proximal and medial zones around the caldera area; p decreases with the distance rather symmetrically around the caldera showing less dependence on vent location with respect to scenario 1. In this latter scenario, the larger p-values may be found within the caldera and in the northern valley, where the caldera rim is breached (Figure 5).

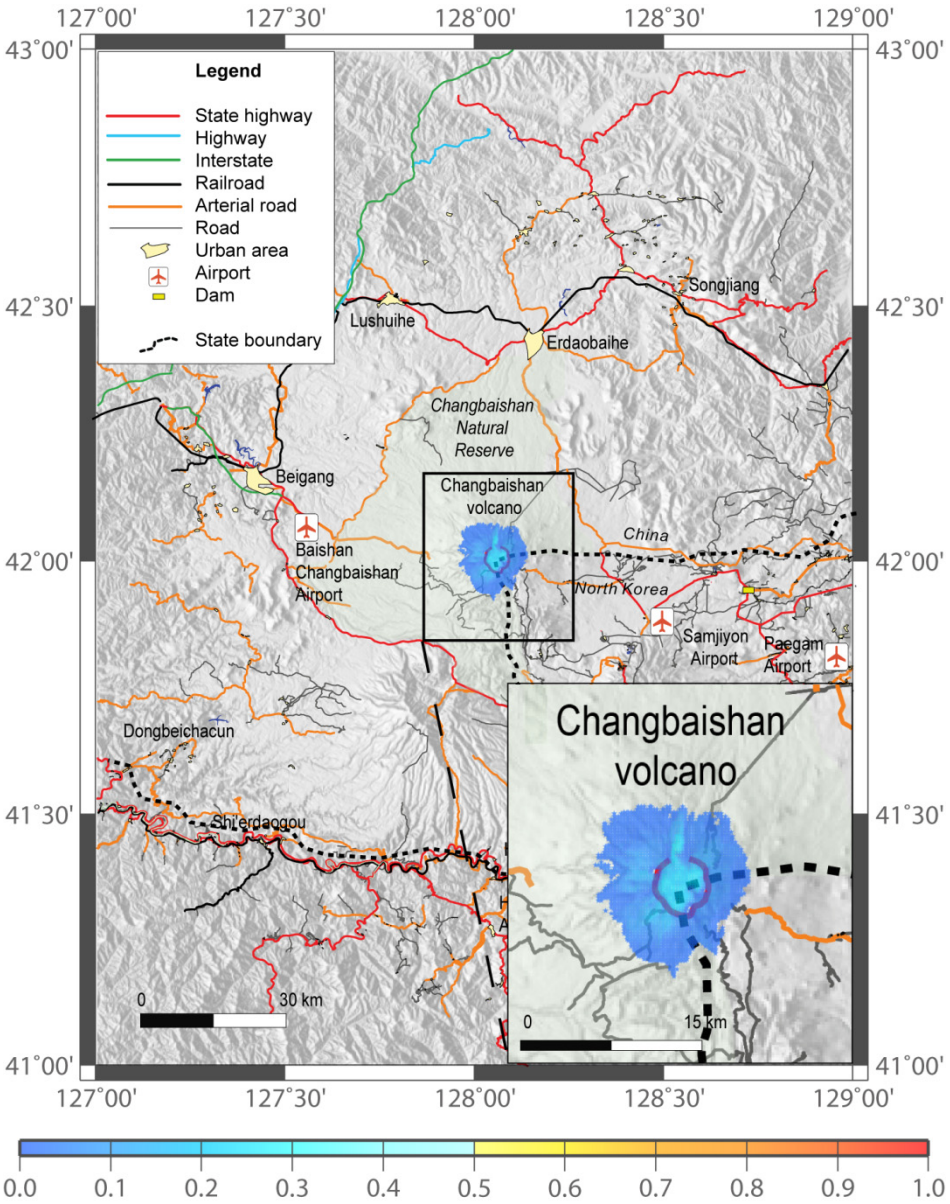

Figure 5. Probability map of invasion by PDCs in scenario 1 (Ht = 3 km) (spatial probability scale at the bottom) superimposed to the China-North Korea infrastructural network; the inset includes a detail of the caldera area.

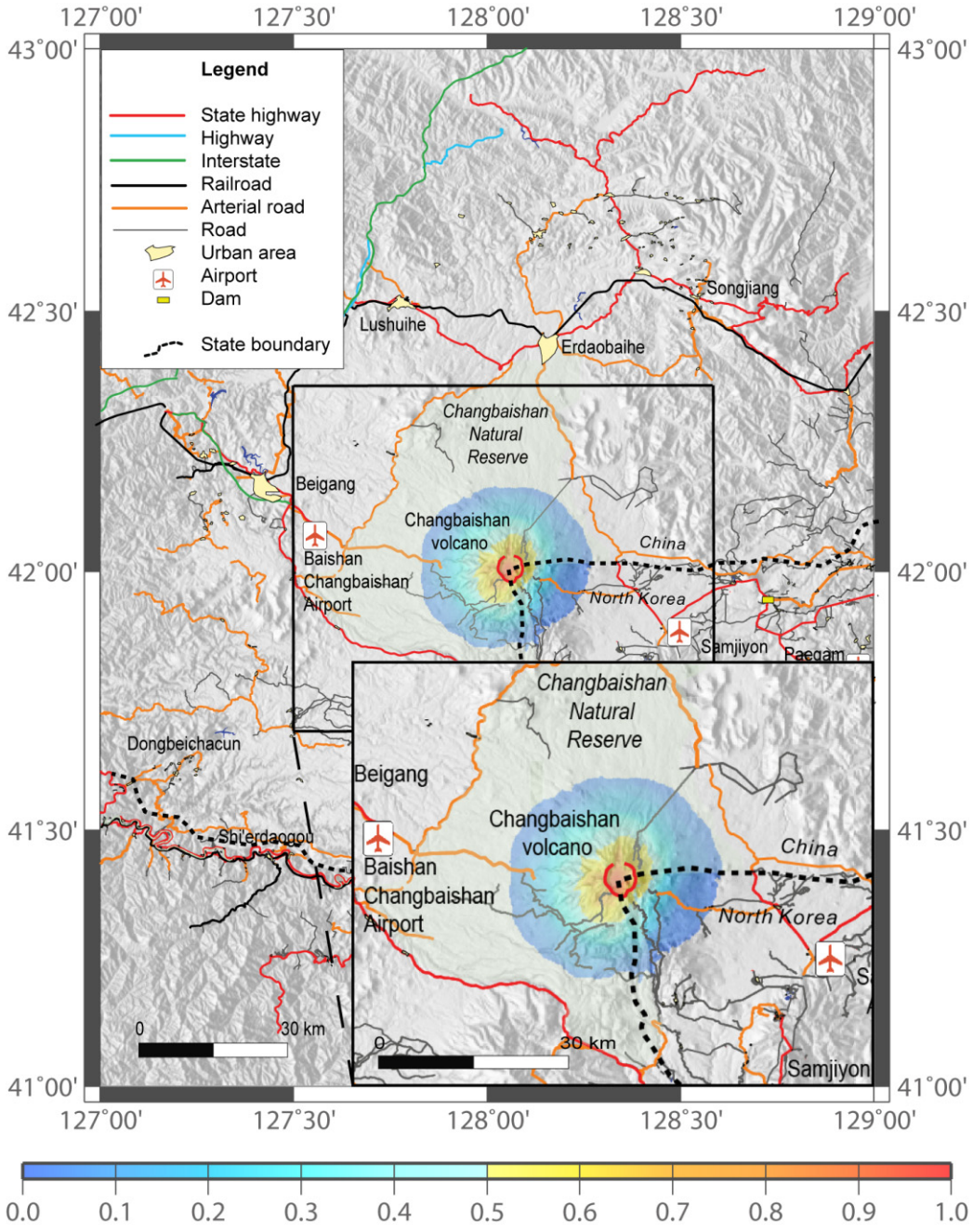

Figure 6. Probability map of invasion by PDCs in scenario 2 (Ht = 10 km) (probability scale at the bottom) superimposed to the China-North Korea infrastructural network; the inset includes a detail of the volcano.

Different types of morphological settings like valleys and walls (caldera rim) influence the deposition and the mobility of PDCs. In scenario 1, only the top of the volcano is potentially affected by PDCs. The area covered by PDC includes the more elevated portion of the Changbaishan Natural Reserve and the road leading to the top of the volcano. In scenario 2, the area with $p \geq 0.5$ characterizes the caldera and the upper, outer flanks of the volcano (Figure 6). The roads connecting China and North Korea located on the southwestern flanks of the volcano are potentially invaded by PDCs. In scenario 3, the area with $p \geq 0.5$ covers the caldera and the upper and lower flanks of the volcano (Figure 7). The whole area of the Changbaishan Natural Reserve is potentially covered by PDC as well as the areas close to the Baishan-Changbaishan (China) and Samjiyon (North Korea) airports.Also, the road leading

to the top of the volcano from Erdaobaihe, along which the Changbashan Observatory instrument building is located, and the Beigang (China)-Heysan (North Korea) state highway are potentially affected by PDCs. In scenarios 4 (Figure 8), the whole volcano, part of the plain and surrounding hills, and the northern sectors of the Wangtian'e and Namphothe strato-volcanoes located south of Changbaishan could be affected by PDCs invasion. All the town and infrastructures (roads, highways, railroads, airports, and dams) can be invaded by PDCs. All the main connections between China and North Korea could be interrupted and the headquarters of the Changbaishan Volcano Observatory and Changbaishan Natural Reserve located in the town of Erdaobaihe would be covered by PDCs.

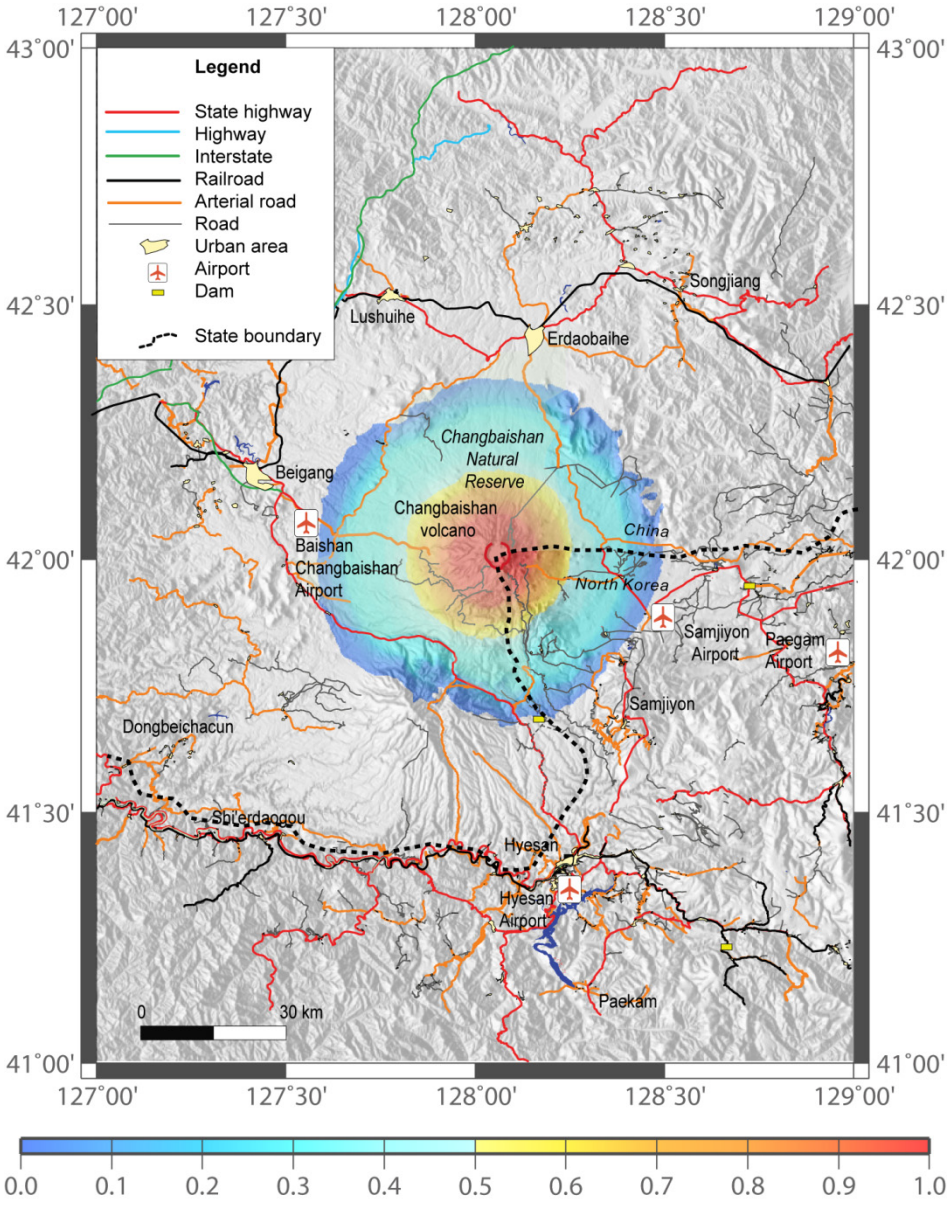

Figure 7. Probability map of invasion by PDCs in scenario 3 (Ht = 20 km) (probability scale at the bottom) superimposed to the China-North Korea infrastructural network.

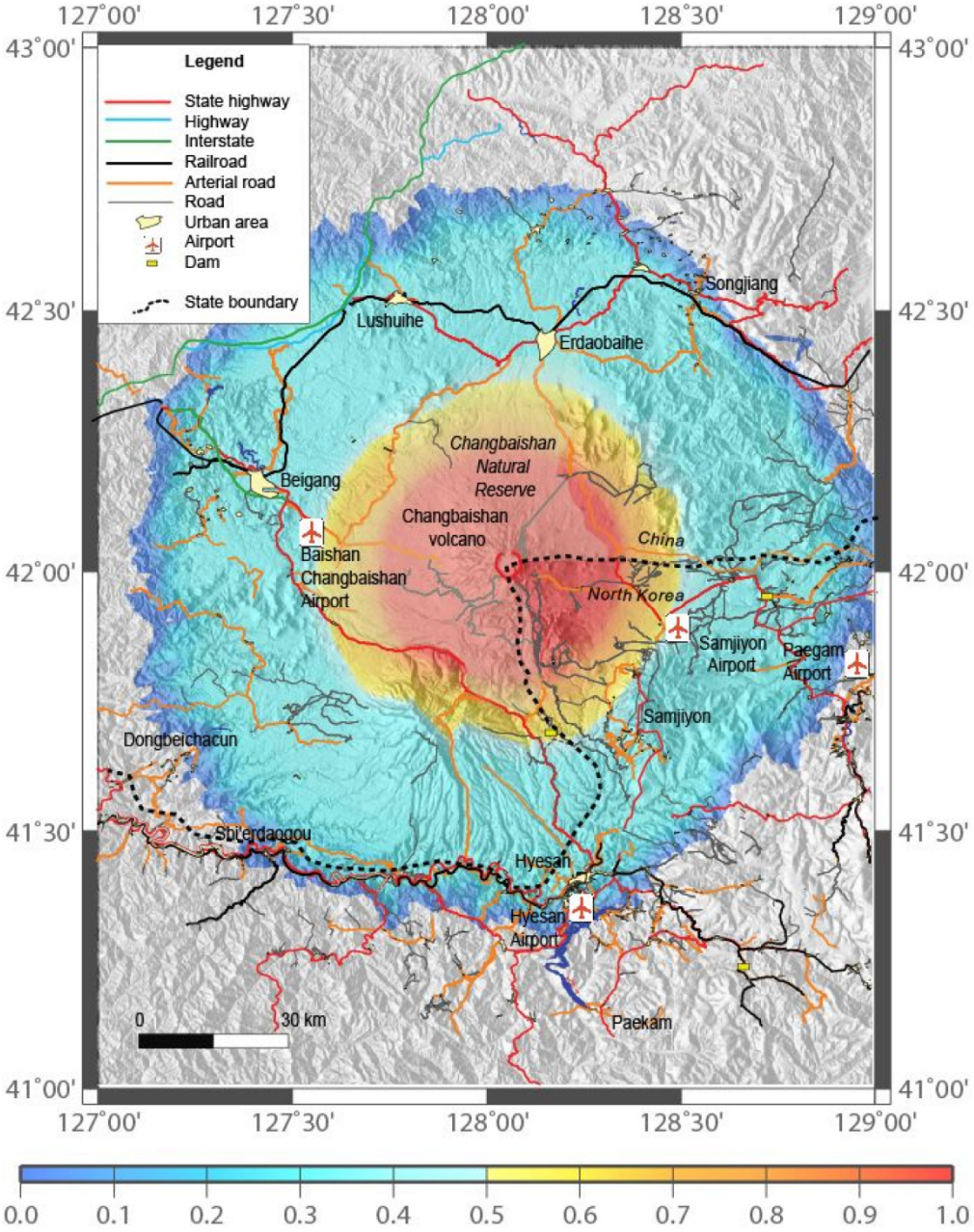

Figure 8. Probability map of invasion by PDCs in scenario 4 (Ht = 30 km) (probability scale at the bottom) superimposed to the China-North Korea infrastructural network.

5. Discussion

The results of the EC runs at Changbaishan show that the areas of invasion from PDCs are influenced by the different vent position only in scenarios 1 and 2. This feature reflects the relatively complex morphology of the top of the volcano.Therefore, we conclude that the up-to-400 m high caldera rim surrounding the Heaven Lake and the caldera breach to the north control the distribution of the PDCs invasion areas on the upper flanks of the volcano, at least for PDCs originated by the collapse of 3–10 km high eruptive columns. The water outlet feeding the Erdaobaihe River could play a role in transforming the potential PDCs flowing in the Erdaobaihe valley in lahars. This conclusion is supported by the field data related to the Millennium eruption, where the PDC-lahar transition has been recognized in the field [51]. Therefore, this type of hazard should also be taken into account at Changbaishan. In the runs, we have assumed that the water of the Heaven Lake does not play a

role in the dynamics of the eruptive column, e.g., magma–water interaction, or PDC flow dynamics. This is a limit of our analysis which cannot be quantified. However, with the exception of vent 1, which is located at the center of the lake, the other 16 vents are located outside the lake area (Figure 3). Our results from runs with the larger ΔH/L values give us a rough estimate of the dispersion areas of potentially denser flows. According to equation 2, the flow mobility is directly expressed by the angle ϕ, a measure of the energy decay rate. This is because larger values of ϕ imply faster energy decay rate and less mobile flows [23]. In this regard, we analyze the relationship between the median, larger and smaller ΔH/L values according to the database of Ogburn [25] and Ogburn and Calder [24], and the distance from the center of the Changbaishan caldera taken as common reference point (Figure 9).

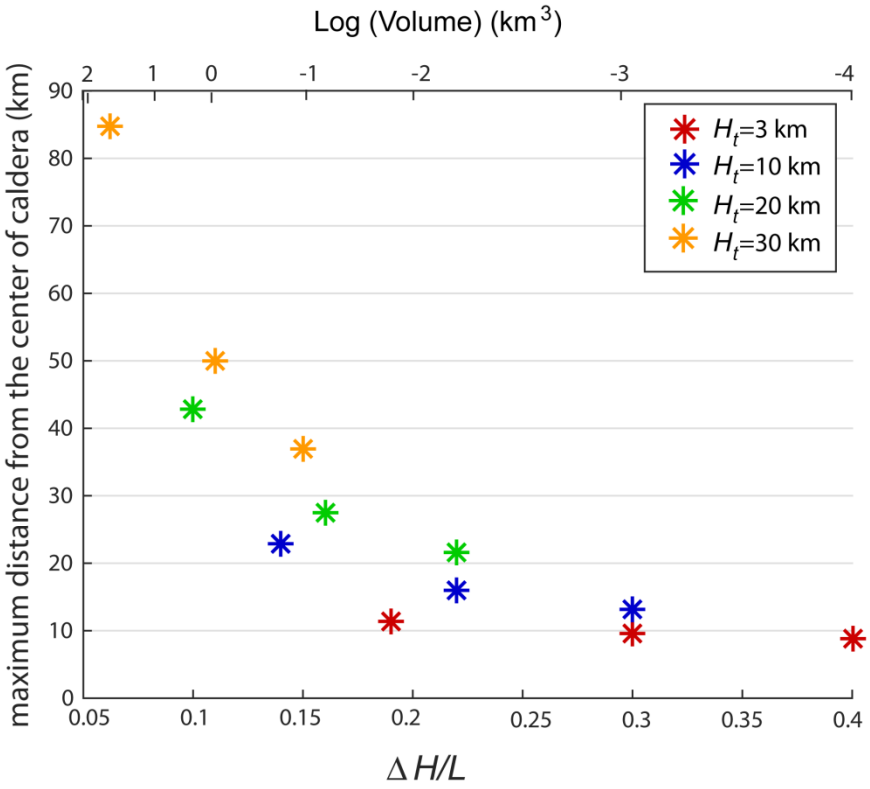

Figure 9. ΔH/L vs. maximum distance from the center of the caldera travelled by PDCs according to the results of simulations in scenarios 1–4. The volumes V corresponding to the selected ΔH/L values are reported and calculated from the equation ΔH/L = 0.11 ($V^{-0.14}$) of [24].

In scenario 1, the maximum distance is within 9–12 km, while in scenario 2, it ranges between 13 and 22 km. In scenarios 3 and 4, the distances are in the ranges 22–42 km and 38–85 km. As shown in Figure 9, this increasing difference between the maximum distances theoretically travelled by PDCs with different ΔH/L values in each scenario does reflect not only the different volumes of PDCs, but also the occurrence of a flat, obstacle-free, topography moving away from the caldera. In addition, the results of the scenario 4 runs (Figure 4) show that some PDCs are potentially able to partly fill the valleys located around the Changbaishan plain in the Gaima basaltic plateau and Sino-Korean Craton (Figure 1). The results of the runs allow us to obtain some empirical relations between the calculated area covered by PDCs and Ht as a function of the different vents and selected ΔH/L. These relations are shown in Figure 10, where the values Ht adopted for the different scenarios are reported versus the areas covered by PDCs. In the diagram, the best-fit lines are obtained by interpolating the minimum, median, and maximum areas values in the different scenarios. These lines, even if obtained by interpolating few points, may be used to obtain an order of magnitude estimate of the area potentially affected by PDC invasion if data on the column height are available and the assumption that PDCs originate by column collapse holds. The empirical relations of Figure 10 clearly show that

the higher the column height, the smaller the difference between the maximum and minimum area potentially affected by PDC. This feature reflects the effects of the topography on the dispersion of PDC, being the areas potentially invaded by PDCs strongly controlled by the relatively complex morphology of the summit portion of the volcano.

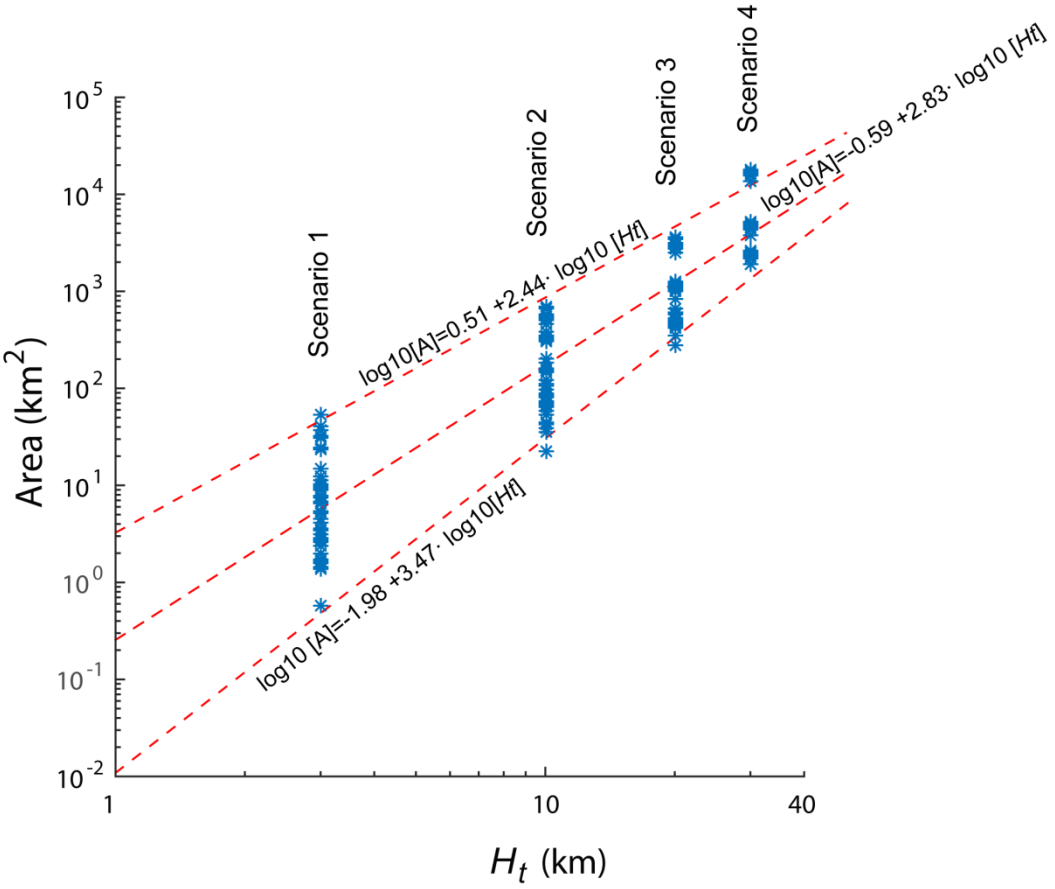

Figure 10. Log-log plots of invasion area (A) versus H_t, for each of the 51 simulations of the scenarios 1–4 and relative linear least square regressions. The regressions are calculated for the median, minimum and maximum values of A in the different scenarios.

In this area, PDCs are expected to be confined within the caldera or valleys, or mantle the outer upper flanks of the volcano, depending on the vent position (see scenarios 1 and 2 in Figure 3). In scenarios 3 and 4, these topographic effects are missing because the plain surrounding Changbaishan is free of relevant morphological obstacles (Figure 1), as previously reported. The variation of the probability of PDC invasion with the distance from the center of the caldera for scenarios 1 and 2 shows that the larger probability is attained at a distance of about 5 km from the caldera and not at its center (Figure 11).

This feature reflects the previously discussed effect of the topography and different vent position on PDC dispersion for these two scenarios, which may be considered representative of small-intermediate eruptions, i.e., Violent Strombolian, Vulcanian, and Subplinian II [39,65]. For the scenarios 3 and 4, which are representative of Sub-Plinian and Plinian eruptions, the probability variation with the distance from the vent for the scenarios 3 and 4 decreases moving away from the caldera with a break at distances of 25–30 km and 42–65 km from the vent, respectively (Figure 11). Here, the probability remains constant ($p = 0.33$), and, at larger distances, decreases. These distances with a $p = 0.33$ constant probability evidence the linear extension of the zones where the simulated PDCs with smaller $\Delta H/L$ regularly superimpose each other (see Figures 7–9). This feature is consistent with the observation that smaller PDCs have a more reduced mobility with respect to the larger ones [32].

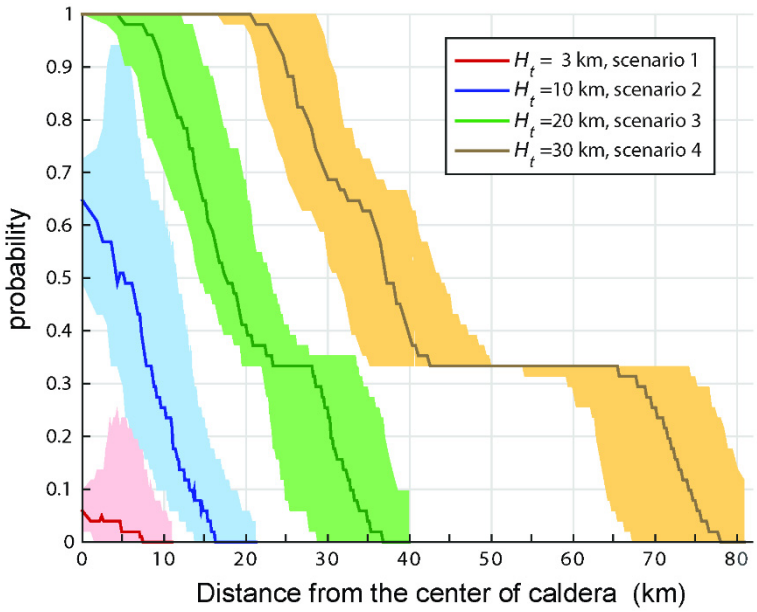

Figure 11. Distance travelled by PDCs from the caldera center vs. conditional probability of invasion.

The results from Figures 2–9 may be used as a guide to evaluate the potential hazard related to PDCs invasion in the case of column collapses from eruptions with VEI 2–7 and Figures 5–8 provide a base to analyze the effects of PDCs invasion on the China and North Korea infrastructural network. In scenarios 1 and 2, only the Changbaishan Natural Reserve, which hosts about 2 milliontourists each year, and the local roads on the upper flanks of the edifice are potentially affected by PDCs. As a result, an interruption of the tourist-related activities with consequent economic loss for the local communities is expected. In scenarios 3 and 4, the Beigang (China)-Heysan (North Korea) state highway, a large part of the residential centers and of the infrastructural network including railroads, airports, and dams could be potentially covered by PDCs. The main limitations of our approach consistofa poor validation of the results due to a lack of knowledge of the timing of volcanic eruptions, their size, and distribution of the products. The latter are available only for the 946 CE 'Millennium' eruption. In that case, our theoretical results of scenario 4 fit the observed distance travelled by PDCs of this eruptionwell. As a result, the main difficulty at Changbaishan is to determinate the frequency of each volcanological event. At present, this lack of data also prevents the use of more sophisticated, probability-based models of hazard map construction [31]. In addition, we do not consider the possible effect of winds on the eruptive column whose collapse may generate PDC. Taking into account these limits, empirical relations between Ht and the PDCs covered area are proposed, and the variation of the expected PDC maximum travelled distance as a function of Ht and ΔH/L is provided. These relations allow us to determine the areas potentially invaded by PDC. Many other PDC invasion maps from column collapses at different height may be provided and the ones presented in our study may be modified.

6. Conclusions

Changbaishan volcano is characterized by a poorly known eruptive history and by a relevant hazard, a condition common to many active volcanoes and volcanic fields worldwide, and, in particular, those located in South America, Asia (e.g., China, Turkey, Saudi Arabia) and Eastern Europe (Caucasus) [66–68]. In this framework, the scenario-based probabilistic approach we adopted for an evaluation of the hazard related to PDCs at Changbaishan, although suffering from afew constraints due to the lack of field data, could be applied to other poorly known and hazardous volcanoes. We produce maps of potential PDCs according to different Ht, PDC volumes and vent location. Probability maps of PDC invasion are also produced for each selected scenario. A contribution of our study is the analysis of the effects of the topography in controlling (or not) the dispersions of PDCs as a function of

volume and column height. Empirical relations between Ht and the PDCs covered area are proposed, and the variation of the expected PDC maximum travelled distance as a function of Ht and ΔH/L is provided. These relations and the produced scenario-based probability maps may be used to evaluate the PDC-related hazard at Changbaishan. Our results make available a working reference frame forexperts of risk mitigation and decision makers.

Author Contributions: G.V. conceived the study, G.V. and P.D.G. run the simulations, A.M.L. provided the statistics and produced the spatial probability maps. Z.G., V.S. and M.Z. contributed to write the text, provided the volcanological background and the data on the infrastructures. G.L. and J.L. provided the volcanological and hazard background. All the authors contributed to write the text. All authors have read and agreed to the published version of the manuscript.

Funding: This study was supported by INGV research funds, and by the Strategic Priority Research Program of Chinese Academy of Sciences (Grant No. XDB26000000), the Key Research Project of Frontier Sciences of Chinese Academy of Sciences (Grant No. QYZDY-SSW-DQC030), and the Natural Science Foundation of China (Grant Nos. 41702361 and 41572321).

Acknowledgments: We thank Xuanlong Shan, Pujun Wang, Jiandong Xu for discussions. G.V. thanks Haiquan Wei for the willingness in providing a lot of his Chinese papers on Changbaishan and Jacopo Taddeucci for a critical reading of an early version of the text and suggestions.

Conflicts of Interest: The authors declare no conflict of interest.

References

1. Wilson, C.J.N. The Taupo eruption, New Zealand II. The Taupo Ignimbrite. *Philos. Trans. R. Soc. Lond. Ser. A* **1985**, *314*, 229–310.
2. Valentine, G.A.; Wohletz, K.H.; Kieffer, S.W. Sources of unsteady column dynamics in pyroclastic flow eruptions. *J. Geophys. Res.* **1991**, *96*, 21887–21892. [CrossRef]
3. Branney, M.J.; Kokelaar, B.P. Pyroclastic density currents and the sedimentation of ignimbrites. *Mem. Geol. Soc. Lond.* **2002**, *27*, 143.
4. Druitt, T.H. Emplacement of the 18 May, 1980 lateral blast deposit east-northeast of Mount St. Helens, Washington. *Bull. Volcanol.* **1992**, *54*, 554–572. [CrossRef]
5. Dufek, J. The fluid mechanics of pyroclastic density currents. *Annu. Rev. Fluid Mech.* **2016**, *48*, 459–485. [CrossRef]
6. Sparks, R.S.J.; Wilson, L. Theoretical modelling of the generation, movement and emplacement of pyroclastic flows by column collapse. *J. Geophys. Res.* **1978**, *B83*, 1727–1739. [CrossRef]
7. Valentine, G.A.; Wohletz, K.H. Numerical models of Plinian eruption columns and pyroclastic flows. *J. Geophys. Res.* **1989**, *94*, 1867–1887. [CrossRef]
8. Hoblitt, R.P. Observations of the eruptions of July 22 and August 7, 1980 at Mount St Helens, Washington. *U.S. Geol. Surv. Prof. Pap.* **1986**, *44*, 1335.
9. Di Roberto, A.; Bertagnini, A.; Pompilio, M.; Bisson, M. Pyroclastic density currents at Stromboli volcano (Aeolian Islands, Italy): A case study of the 1930 eruption. *Bull. Volcanol.* **2014**, *76*, 827. [CrossRef]
10. Houghton, B.F.; Wilson, C.J.N.; Fierstein, J.; Hildreth, W. Complex proximal deposition during the Plinian eruptions of 1912 at Novarupta, Alaska. *Bull. Volcanol.* **2004**, *66*, 95–133. [CrossRef]
11. Komorowski, J.-C.; Jenkins, S.; Baxter, P.J.; Picquot, A.; Lavigne, F.; Charbonnier, S.; Gertisser, R.; Preece, K.; Cholik, N.; Budi-Santoso, A. Paroxysmal dome explosion during the Merapi 2010 eruption processes and facies relationships of associated high-energy pyroclastic density currents. *J. Volcanol. Geotherm. Res.* **2013**, *261*, 260–294. [CrossRef]
12. Nairn, I.A.; Self, S. Explosive eruptions and pyroclastic avalanches from Ngauruhoe in February 1975. *J. Volcanol. Geotherm. Res.* **1978**, *3*, 39–60. [CrossRef]
13. Dufek, J.; Bergantz, G.W. Suspended load and bed-load transport of particle-laden gravity currents: The role of particle-bed interaction. *Comp. Fluid Dyn.* **2007**, *21*, 119–145. [CrossRef]
14. Roche, O. Depositional processes and gas pore pressure in pyroclastic flows: An experimental perspective. *Bull. Volcanol.* **2012**, *74*, 1807–1820. [CrossRef]

15. Esposti-Ongaro, T.; Clarke, A.B.; Voight, B.; Neri, A.; Widiwijayanti, C. Multiphase flow dynamics of pyroclastic density currents during the May 18, 1980 lateral blast of Mount St. Helens. *J. Geophys. Res.* **2012**, *117*, B06208. [CrossRef]
16. Andrews, B.J. Dispersal and air entrainment in unconfined dilute pyroclastic density currents. *Bull. Volcanol.* **2014**, *76*, 852. [CrossRef]
17. Breard, E.; Lube, G. Inside pyroclastic density currents–uncovering the enigmatic flow structure and transport behaviour in large-scale experiments. *Earth Planet. Sci. Lett.* **2017**, *458*, 22–36. [CrossRef]
18. Auker, M.R.; Sparks, R.S.J.; Siebert, L.; Crosweller, H.S.; Ewert, J. A statistical analysis of the global historical volcanic fatalities record. *J. Appl. Volcanol.* **2013**, *2*, 2. [CrossRef]
19. Brown, S.K.; Jenkins, S.F.; Sparks, R.S.J.; Odbert, H.; Auker, M.R. Volcanic fatalities database: Analysis of volcanic threat with distance and victim classification. *J. Appl. Volcanol.* **2017**, *6*, 15. [CrossRef]
20. Kelfoun, K.; Druitt, T.H. Numerical modeling of the emplacement of Socompa rock avalanche, Chile. *J. Geophys. Res.* **2005**, *110*, 1–13. [CrossRef]
21. Iverson, R.M.; Schilling, S.P.; Vallance, J.W. Objective delineation of lahar-inundation hazard zones. *Geol. Soc. Am. Bull.* **1998**, *110*, 972–984. [CrossRef]
22. Pitman, E.B.; Nichita, C.C.; Sheridan, M.F.; Patra, A.K.; Bauer, A.C.; Bursik, M.I. Computing granular avalanches and landslides. *Phys. Fluids* **2003**, *15*, 3638. [CrossRef]
23. Malin, M.C.; Sheridan, M.F. Computer-assisted mapping of pyroclastic surges. *Science* **1982**, *217*, 637–640. [CrossRef] [PubMed]
24. Ogburn, S.E.; Calder, E.S. The relative effectiveness of empirical and physical models for simulating pyroclastic density currents under different emplacement conditions. *Front. Earth Sci.* **2017**, *5*, 83. [CrossRef]
25. Ogburn, S.E. *Flowdat—Mass Flow Database: Vhub Database*; 2012 (Virginia, USA). Available online: https://vhub.org/groups/massflowdatabase (accessed on 12 December 2019).
26. Ui, T. Volcanic dry avalanche deposits-Identification and comparison with non-volcanic debris stream deposits. *J. Volcanol. Geotherm. Res.* **1983**, *18*, 135–150. [CrossRef]
27. Hayashi, J.N.; Self, S. A comparison of pyroclastic flow and debris avalanche mobility. *J. Geophys. Res.* **1992**, *97B6*, 9063–9071. [CrossRef]
28. Sheridan, M.F.; Macías, J.L. Estimation of risk probability for gravity-driven pyroclastic flows at Volcán Colima, México. *J. Volcanol. Geotherm. Res.* **1995**, *66*, 251–256. [CrossRef]
29. Takarada, S. The volcanic hazards assessment support system for the online hazard assessment and risk mitigation of Quaternary volcanoes in the world. *Front. Earth Sci.* **2017**, *5*, 102. [CrossRef]
30. Alberico, I.; Lirer, L.; Petrosino, P.; Scandone, R. A methodology for the evaluation of long-term volcanic risk from pyroclastic fows in Campi Flegrei (Italy). *J. Volcanol. Geotherm. Res.* **2002**, *116*, 63–78. [CrossRef]
31. Tierz, P.; Sandri, L.; Costa, A.; Zaccarelli, L.; Di Vito, M.A.; Sulpizio, R.; Marzocchi, W. Suitability of energy cone for probabilistic volcanic hazard assessment: Validation tests at Somma-Vesuvius and Campi Flegrei (Italy). *Bull. Volcanol.* **2016**, *78*, 79. [CrossRef]
32. Ogburn, S.E.; Berger, J.; Calder, E.S.; Lopes, D.; Patra, A.; Pitman, E.B.; Rutarindwa, R.; Spiller, E.; Wolpert, R.L. Pooling strength amongst limited datasets using hierarchical Bayesian analysis, with application to pyroclastic density current mobility metrics. *Stat. Volcanol.* **2016**, *2*, 1–26. [CrossRef]
33. Oppenheimer, C.; Wacker, L.; Xu, J.; Galván, J.D.; Stoffel, M.; Guillet, S.; Corona, C.; Sigl, M.; Di Cosmo, N.; Hajdas, I.; et al. Multi-proxy dating the 'Millennium Eruption' of Changbaishan to late 946 CE. *Quat. Sci. Rev.* **2017**, *158*, 164–171. [CrossRef]
34. Horn, S.; Schmincke, H.U. Volatile emission during the eruption of Baitoushan volcano (China/North Korea) ca. 969 AD. *Bull. Volcanol.* **2000**, *61*, 537–555. [CrossRef]
35. Zou, H.; Fan, Q.; Zhang, H. Rapid development of the great Millennium eruption of Changbaishan (Tianchi) Volcano, China/North Korea: Evidence from U-Th zircon dating. *Lithos* **2010**, *119*, 289–296. [CrossRef]
36. Wei, H.; Liu, G.; Gill, J. Review of eruption activity at Tianchi volcano, Changbaishan, northeast China: Implications for possible future eruptions. *Bull. Volcanol.* **2013**, *75*, 705–719. [CrossRef]
37. Pan, B.; de Silva, S.L.; Xu, J.; Chen, Z.; Miggins, D.P.; Wei, H. The VEI-7 Millennium eruption, Changbaishan-Tianchi volcano, China/DPRK: New field, petrological, and chemical constraints on stratigraphy, volcanology, and magma dynamics. *J. Volcanol. Geotherm. Res.* **2017**, *343*, 45–59. [CrossRef]

38. Xu, J.; Liu, G.; Wu, J.; Ming, Y.; Wang, Q.; Cui, D.; Shangguan, Z.; Pan, B.; Lin, X.; Liu, J. Recent unrest of Changbaishan volcano, Northeast China: A precursor of a future eruption. *Geophys. Res. Lett.* **2012**, *39*, L16305. [CrossRef]
39. Bonadon na, C.; Costa, A. Plume height, volume, and classification of explosive volcanic eruptions based on the Weibull function. *Bull. Volcanol.* **2013**, *75*, 742. [CrossRef]
40. Wei, H.; Sparks, R.S.J.; Liu, R.; Fan, Q.; Wang, Y.; Hong, H.; Zhang, H.; Chen, H.; Jiang, C.; Dong, J.; et al. Three active volcanoes in China and their hazards. *J. Asian Earth Sci.* **2003**, *21*, 515–526. [CrossRef]
41. Zhang, M.; Guo, Z.; Liu, J.; Liu, G.; Zhang, L.; Lei, M.; Zhao, W.; Ma, L.; Sepe, V.; Ventura, G. The intraplate Changbaishan volcanic field (China/North Korea): A review on eruptive history, magma genesis, geodynamic significance, recent dynamics and potential hazards. *Earth Sci. Rev.* **2018**, *187*, 19–52. [CrossRef]
42. Liu, R.; Wei, H.; Li, J. *The Recent Eruptions of Changbaishan Tianchi Volcano*; Science Press: Beijing, China, 1998; pp. 1–159. (In Chinese)
43. Fan, Q.; Sui, J.; Wang, T.; Li, N.; Sun, Q. History of volcanic activity, magma evolution and eruptive mechanisms of the Changbai volcanic province. *Geol. J. China Univ.* **2007**, *13*, 175–190, (In Chinese with English abstract).
44. Wei, H.; Wang, Y.; Jin, J.; Gao, L.; Yun, S.-H.; Jin, B. Timescale and evolution of the intracontinental Tianchi volcanic shield and ignimbrite-forming eruption, Changbaishan. Northeast China. *Lithos* **2007**, *96*, 315–324. [CrossRef]
45. Cui, Z.; Wei, H.; Liu, R. A Textual Research on the Historic Records of the Eruptions from Tianchi Volcano, Changbaishan. In *Connection of Volcanism and Human Environment*; Liu, R., Ed.; Seismic Press: Beijing, China, 1995; pp. 36–39.
46. Zhao, B.; Xu, J.; Lin, C. Study of distal pyroclastic-flow stratum from Tianchi volcano in 1215±15 eruption pyroclastic-flow over water. *Acta Geol. Sin. Engl.* **2013**, *87*, 73–81.
47. Yang, L.; Wang, F.; Feng, H.; Wu, L.; Shi, W. 40Ar/39Ar geochronology of Holocene volcanic activity at Changbaishan Tianchi volcano, Northeast China. *Quat. Geochronol.* **2014**, *21*, 106–114. [CrossRef]
48. Sun, C.; Liu, J.; You, H.; Nemeth, K. Tephrostratigraphy of Changbaishan volcano, northeast China, since the mid-Holocene. *Quat. Sci. Rev.* **2017**, *177*, 104–119. [CrossRef]
49. Sun, C.; Wang, L.; Plunkett, G.; You, H.; Zhu, Z.; Zhang, L.; Zhang, B.; Chu, G.; Liu, J. Ash from the Changbaishan Qixiangzhan eruption: A new early Holocene marker horizon across East Asia. *J. Geophys. Res. Solid Earth* **2018**, *123*, 6442–6450. [CrossRef]
50. McLean, D.; Albert, P.G.; Nakagawa, T.; Staff, R.A.; Suzuki, T.; Suigetsu Smith, V.C. Identification of the Changbaishan "Millennium" (B-Tm) eruption deposit in the Lake Suigetsu (SG06) sedimentary archive, Japan: Synchronisation of hemispheric-wide palaeoclimate archives. *Quat. Sci. Rev.* **2016**, *150*, 301–307. [CrossRef]
51. Liu, X.; Xiang, T. *Cenozoic Volcanoes and Pyroclastic Deposits in Northeastern China: Resources and Hazards*; Jilin Univ Publishing House: Changchun, China, 1997; p. 161. (In Chinese)
52. Choi, S.; Oh, C.W.; Gotze, H.J. Three-dimensional density modeling of the EGM2008 gravity field over the Mount Paekdu volcanic area. *J. Geophys. Res. Solid Earth* **2013**, *118*, 3820–3836. [CrossRef]
53. Wu, J.; Ming, Y.; Fang, L.; Wang, W. S-wave velocity structure beneath Changbaishan volcano inferred from receiver function. *Earthq Sci.* **2009**, *22*, 409–416. [CrossRef]
54. Wei, H.; Hong, H.; Sparks, R.S.J.; Walder, J.S.; Han, B. Potential hazards of eruptions around the Tianchi caldera lake, China. *Acta Geol. Sin.* **2004**, *78*, 790–794.
55. Dai, L.; Wang, Y.; Lewis, B.J.; Xu, D.; Zhou, L.; Gu, X.; Jiang, L. The trend of land-use sustainability around the Changbai Mountain Biosphere Reserve in northeastern China: 1977–2007. *Int. J. Sust. Dev. World* **2012**, *19*, 369–377. [CrossRef]
56. National Bureau of Statistics of China. Popul. Census 2010. 2012. Available online: https://www.stats.gov.cn (accessed on 23 April 2013). (In Chinese)
57. Lee, S.-H.; Jang, E.-S.; Lee, H.-M. A case analysis of volcanic ash dispersion under various volcanic explosivity index of the Mt. Baegdu. *J. Korean Earth Sci. Soc.* **2012**, *33*, 280–293. (In Korean) [CrossRef]
58. Yu, H.; Xu, J.; Luan, P.; Zhao, B.; Pan, B. Probabilistic assessment of tephra fallout hazard at Changbaishan volcano, Northeast China. *Nat. Hazards* **2013**, *69*, 1369–1388. [CrossRef]

59. Yu, S.; Yoon, S.M.; Choi, E.K.; Kim, S.D.; Lee, Y.J.; Lee, Y.; Choi, K.H. Quantitative assessment of national resilience: A case study of Mount Paektu eruption scenarios on South Korea. *Int. J. Disast Risk Reduct.* **2016**, *19*, 118–132. [CrossRef]
60. Yun, S.H.; Lee, J.H.; Kim, S.K.; Chang, C.W.; Cho, E.; Yang, I.S.; Kim, Y.J.; Kim, S.H.; Lee, K.H.; Kim, S.W.; et al. TITAN2D simulations of pyroclastic flows from small scale eruption at Mt. Baekdusan. *J. Korean Earth Sci. Soc.* **2013**, *34*, 615–625, (In Korean with English abstract). [CrossRef]
61. Paone, A.; Yun, S.-H. Pyroclastic Density Current Hazards at the Baekdusan Volcano, Korea: Analyses of Several Scenarios from a Small-Case to the Worst-Case Colossal Eruption. In *Updates in Volcanology-From Volcano Modelling to Volcano Geology*; InTech press: London, UK, 2016.
62. Heim, A. *Bergsturz und Menschenleben*; Fretz und Wasmuth: Zurich, Switzerland, 1932; Volume 218. (In German)
63. Newhall, C.G.; Self, S. The volcanic explosivity index (VEI): An estimate of explosive magnitude for historical volcanism. *J. Geophys. Res.* **1992**, *87*, 1231–1238. [CrossRef]
64. Mastin, L.G.; Guffanti, M.; Servranckx, R.; Webley, P.; Barsotti, S.; Dean, K.; Durant, A.; Ewert, J.W.; Neri, A.; Rose, W.I.; et al. A multidisciplinary effort to assign realistic source parameters to models of volcanic ash-cloud transport and dispersion during eruptions. *J. Volcanol. Geotherm. Res.* **2009**, *186*, 10–21. [CrossRef]
65. Cioni, R.; Bertagnini, A.; Santacroce, R.; Andronico, D. Explosive activity and eruption scenarios at Somma-Vesuvius (Italy): Towards a new classification scheme. *J. Volcanol. Geotherm. Res.* **2008**, *178*, 331–346. [CrossRef]
66. Németh, K. Monogenetic volcanic fields: Origin, sedimentary record, and relationship with polygenetic volcanism. In: E. Cañón-Tapia and A. Szakács (Editors), What is a volcano? *Geol. Soc. Am.* **2010**, *470*, 43–66.
67. Neri, M.; Le Cozannet, G.; Thierry, P.; Bignami, C.; Ruch, J. A method for multi-hazard mapping in poorly known volcanic areas: An example from Kanlaon (Philippines). *Nat. Hazards Earth Syst. Sci.* **2013**, *13*, 1929–1943. [CrossRef]
68. Németh, K.; Kereszturi, G. Monogenetic volcanism: Personal views and discussion. *Int. J. Earth Sci.* **2015**, *104*, 2131–2146. [CrossRef]